SUPERNOVA EXPLOSIONS IN DEGENERATE STARS
---DETONATION, DEFLAGRATION, AND ELECTRON CAPTURE---

Ken'ichi Nomoto*
Laboratory for Astronomy and Solar Physics
NASA/Goddard Space Flight Center
Greenbelt, MD 20771, USA

ABSTRACT

Presupernova evolution and the hydrodynamic behavior of supernova explosions in stars having electron-degenerate cores are summarized. Carbon deflagration supernovae in C+O cores disrupt the star completely. On the other hand, in electron capture supernovae, O+Ne+Mg cores collapse to form neutron stars despite the competing oxygen deflagration.

Also discussed are white dwarf models for Type I supernovae (SN I). Supernova explosions in accreting white dwarfs are either the detonation or deflagration type depending mainly on the accretion rate. The carbon deflagration model reproduces many of the observed features of SN I.

1. INTRODUCTION

Electron degeneracy in the stellar interior has a strong influence on the structure and evolution of small and intermediate mass stars, which has been investigated as a fundamental problem since Chandrasekhar (1939). In the final stages of evolution, electron degeneracy provides several triggering mechanisms of supernova explosions. Supernovae in normal red giant stars forming degenerate cores probably contribute to a major fraction of the total rate of Type II supernovae (SN II) and neutron star formation in the Galaxy. Also, it has been suggested that Type I supernovae (SN I) are related to degenerate stars with no hydrogen-rich envelope. However, we have not yet reached agreement about either the final fates of such stars (total disruption or neutron star formation) or the origin of SN I.

In this review, we summarize the recent efforts and achievements in the above problems; the following types of supernovae are discussed. (1) A thermonuclear explosion in a degenerate core was proposed as one of the triggering mechanisms of supernovae by Hoyle and Fowler (1960).

*On leave from Department of Physics, Ibaraki University, Japan

D. Sugimoto, D. Q. Lamb, and D. N. Schramm (eds.), Fundamental Problems in the Theory of Stellar Evolution, 295–315.

Many computations have shown that this type of explosion occurs as a carbon deflagration supernova in stars of mass $6 \pm 2 < M/M_\odot < 8 \pm 1$ (Arnett 1969; Nomoto et al. 1976).

(2) Electron captures have also been suggested to trigger the collapse of degenerate cores (Rakavy et al. 1967). However, little has been known about the presupernova evolution and the hydrodynamic behavior of this type of supernovae until the recent computations by Miyaji et al. (1980) and Nomoto (1980a). They showed that stars of 8 to 10 $M_\odot$ evolve into electron cpature supernovae in which the degenerate O+Ne+Mg core collapses to form neutron stars.

(3) White dwarfs have been thought to be candidates for SN I because of the absence of hydrogen lines in their spectrum and their appearance in elliptical galaxies (Finzi and Wolf 1967). Recent progress in the radioactive decay model for the light curve of SN I (Colgate et al. 1980) has renewed the interest in the detonation/deflagration type supernovae in the accreting white dwarfs.

2. EVOLUTION OF DEGENERATE CORES

In the advanced phases of evolution, electrons become degenerate in a core of He, C+O, and O+Ne+Mg for the stars of mass smaller than about 2 $M_\odot$, 8 $M_\odot$, and 10 $M_\odot$, respectively. Since the pressure depends only slightly on temperature in the equation of state of degenerate electrons, onset of electron degeneracy changes the global thermodynamics of the core as a self-gravitating system, i.e., the sign of the gravothermal specific heat changes from negative to positive (e.g. Kippenhahn 1970; Hachisu and Sugimoto 1978). As a result, the star evolves in the following way, which differs greatly from the more massive stars evolving into gravitational collapse.

2.1 Critical Core Mass for Non-Degenerate Ignition

During the gravitational contraction of the partially degenerate core, the temperature attains its maximum and then decreases by emitting photons and neutrinos. Such a maximum temperature is obtained for the core of a fixed mass, and its value is lower if the core mass is smaller. This implies that there exists a certain critical core mass for nuclear burning to be initiated under non-degenerate or partially-degenerate condition. Such critical core masses are 0.08 $M_\odot$ (Kumar 1963), 0.31 $M_\odot$ (Cox and Salpeter 1964), 1.06 $M_\odot$ (Murai et al. 1968), and 1.37 $M_\odot$ (Boozer et al. 1973) for the ignition of hydrogen, helium, carbon, and neon, respectively.

In the actual evolution, the core mass increases because materials in the envelope flow into the core through the nuclear burning shell. As an example, let us discuss the C+O core. (Hereafter M_H, M_{He}, and M_C, denote the core mass contained interior to the burning shell of hydrogen, helium and carbon, respectively.) In a star of mass $M > (8 \pm 1)M_\odot$, the mass of the C+O core, M_{He}, reaches the critical core mass 1.06 $M_\odot$ before the electron degeneracy sets in so that carbon burning proceeds under

non-degenerate condition. For a smaller mass star, on the other hand, M_{He} is smaller than 1.06 $M_\odot$ when the maximum temperature is attained. Accordingly non-degenerate ignition does not occur and the cool electron-degenerate C+O core is formed.

2.2 Development of Degenerate C+O Core

The evolutionary path of such a degenerate C+O core in the central density ρ_c and temperature T_c plane is shown in Figure 1, which was computed from the helium burning through the carbon ignition for the helium core of initial mass $M_H^{(0)} = 1.5\ M_\odot$ in the 7 $M_\odot$ star (Sugimoto and Nomoto 1975; see also Rose 1969, Paczyński 1970). As is well-known, evolution of the intermediate mass stars converges to the same track in this plane irrespective of their total mass (Paczyński 1970), becuase it is determined only by the competition between the growth rate of M_{He} ($\simeq M_H$) due to the H/He double shell-burnings and the neutrino cooling rate. Carbon burning is ignited at $\rho_c \simeq 2.5 \times 10^9$ g cm^{-3} and grows into the flash because of the positive specific heat of the degenerate matter. This is the trigger of the carbon deflagration supernova.

Details of such an evolution are seen in the recent reviews by Sugimoto and Nomoto (1980) and Mazurek and Wheeler (1980). It should be noted that the mass range of the star which evolves through the carbon deflagration would be roughly $(6 \pm 2 - 8 \pm 1)M_\odot$ but is very uncertain because it depends on the mass loss in the red giant stages (see e.g. Wheeler 1978b) and also on chemical composition (Alcock and Paczyński 1978; Becker and Iben 1979).

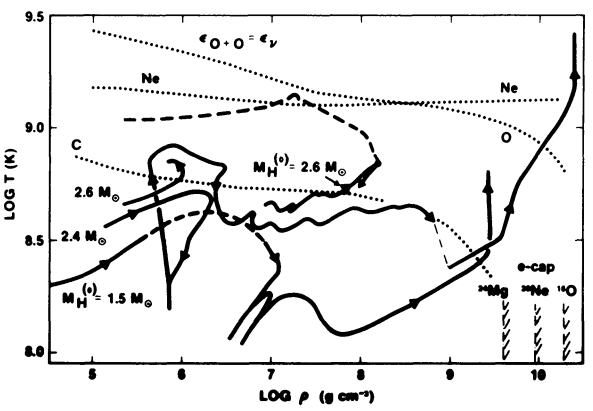

Figure 1. Evolution of the central density and temperature for the helium core of initial mass $M_H^{(0)} = 1.5\ M_\odot$, 2.4 $M_\odot$, and 2.6 $M_\odot$ (solid). Dashed line for the 2.6 $M_\odot$ core shows a structure from the center toward the core edge at the off-center Ne ignition. Dotted are ignition lines for C, Ne, and O, and dot-dashed are the threshold densities for electron captures.

2.3 Formation of Degenerate O+Ne+Mg Core

In stars of $M > (8 \pm 1)M_\odot$, O+Ne+Mg core is formed after the stable carbon burning. If we apply the same discussion in section 2.1 to this core, we can expect that there exists a mass range for which a degenerate

https://doi.org/10.1017/S0074180900074106 Published online by Cambridge University Press

O+Ne+Mg core is formed. Although the stars in this mass range would be the progenitors of most of neutron stars (Barkat et al. 1974; Wheeler 1978b), little attention has been paid to the evolution beyond the carbon burning until quite recently.

This expectation was recently confirmed by Nomoto (1980a) and Miyaji et al. (1980). Nomoto (1980a) computed the evolution of helium cores of initial masses $M_H^{(0)} = 2.4\ M_\odot$ and $2.6\ M_\odot$ starting at the helium burning stage. These cores correspond to the stellar mass of $(10 \pm 1) M_\odot$ depending on the mass loss and chemical compositions. Evolutionary paths of the central density and temperature for both cases and chemical evolution of the $2.4\ M_\odot$ core are shown in Figures 1 and 2, respectively. The core of $M_H^{(0)} = 2.4\ M_\odot$ evolves through the following stages.

(1) Carbon burning in non-degenerate core: Carbon is ignited off-center, and then the burning layer shifts inward due to heat conduction and reaches the center as seen in Figure 2. This is similar to the result by Boozer et al. (1973) and Ergma and Vilhu (1978). Afterwards carbon burning proceed in non-degenerate condition at $\rho_C \sim 10^6 \mathrm{g\ cm^{-3}}$ (Figure 1).

(2) Growth of O+Ne+Mg core: The resultant O+Ne+Mg core of mass M_C grows through the phases of several carbon-shell flashes (Figure 2). These shell flashes are mild; the peak energy generation rate attained is only $L_{C+C} = 2 \times 10^7\ L_\odot$. In this core, a temperature inversion appears. After a maximum temperature of 1.13×10^9K is attained in the shell of $M_r = 1.26\ M_\odot$, the temperature begins to decrease because of the neutrino loss. Neon ignition does not occur (see the ignition line of $\varepsilon_{Ne} = \varepsilon_\nu$ in Figure 1) because $M_{He} = 1.343\ M_\odot$ is smaller than the critical mass of $1.37\ M_\odot$ for the neon ignition (Boozer et al. 1973). The electron degeneracy becomes stronger as M_C increases.

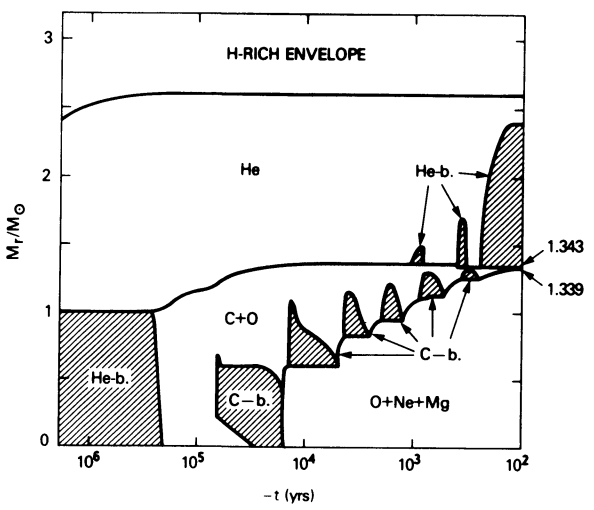

Figure 2. Chemical evolution for the star of $M_H^{(0)} = 2.4\ M_\odot$.

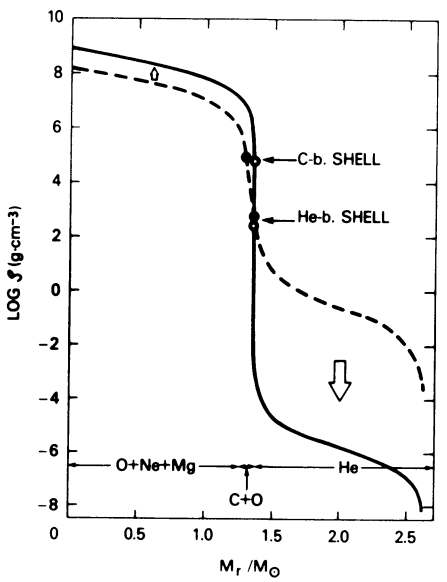

Figure 3. Expansion of the helium zone at the end stage in Figure 2.

https://doi.org/10.1017/S0074180900074106 Published online by Cambridge University Press

(3) Expansion of helium zone and penetration of the surface convection zone: When M_C reaches 1.339 $M_\odot$ which is very close to M_{He} (=1.343 $M_\odot$), the helium zone expands greatly as seen in Figure 3. This is the same phenomenon as occurs in the 2 $M_\odot$ helium star having the degenerate C+O core (Paczyński 1971). The mechanism of such expansion is the same as when a main-sequence star becomes a red giant star (cf. Sugimoto and Nomoto 1980). The temperature at the core edge drops to 10^4K which implies that the surface convection zone would penetrate into the helium zone if the hydrogen-rich envelope were taken into account in the computation (cf. Becker and Iben 1979). The mass M_H will be reduced down to $M_H \simeq 1.343\ M_\odot$, and the star will have very thin helium and carbon zones.
(4) Core growth by triple shell-burning: After that the O+Ne+Mg core will grow toward the Chandrasekhar limit through the phases of triple shell-burning of hydrogen, helium, and carbon, which would be almost the same as the growth of the C+O core by the double shell-burnings. Therefore evolution of 8 to 10 $M_\odot$ stars in $\rho_C - T_C$ Plane will converge to the same track. The ultimate fate of such stars is an electron capture supernova (Miyaji et al. 1980) as will be discussed in section 4.

2.4 Off-Center Neon Burning

In the core of $M_H^{(0)} = 2.6\ M_\odot$, carbon is ignited in the center. Subsequent evolution of the growing O+Ne+Mg core through the phases of carbon shell-flashes are qualitatively the same as in the core of $M_H^{(0)} = 2.4\ M_\odot$. However, M_{He} reaches 1.45 $M_\odot$ exceeding the critical mass of 1.37 $M_\odot$, so that neon is ignited off-center as seen from the structure line (dashed) in Figure 1. Peak energy generation rate reaches $L_{Ne} = 3 \times 10^{13} L_\odot$ but no dynamical effect is induced.

The inward shift of such neon/oxygen burning shell was computed for the 8 $M_\odot$ star having core of $M_{He} \simeq 1.4\ M_\odot$ (Barkat et al. 1974) and for the C+O star of $M_{He} = 1.5\ M_\odot$ (Ikeuchi et al. 1972). The result depends on M_{He}: A degenerate O+Ne+Mg core of 0.3 $M_\odot$ remains unburned in the former case, while neon burning-shell reaches the center and a degenerate Si core is formed in the latter.

Recently, the evolution of a 10 $M_\odot$ star was computed up to the supernova stage by Weaver and Woosley (1979). In their model, $M_{He} \simeq 1.55\ M_\odot$ so that neon is ignited and a deflagration wave develops. Helium and hydrogen layers are then ejected and the resultant 1.55 $M_\odot$ core evolves into the phase of iron core collapse to form a neutron star.

These results show that the evolution in the mass range of (10 ± 1) to $(12 \pm 1) M_\odot$ is quite sensitive to stellar mass because the C+O core mass, M_{He}, varies from 1.37 $M_\odot$ to 1.6 $M_\odot$ crossing the Chandrasekhar limit. In other words, such a mass range corresponds to the transition from degenerate to non-degenerate stars.

3. CARBON DEFLAGRATION SUPERNOVAE

The ultimate fate of the stars having degenerate C+O core has been extensively investigated since Arnett (1969) proposed a model of carbon detonation supernova. We discuss some basic problems in the detonation/deflagration models which can also be applied to the white dwarf models for SN I (section 5). (See details in Sugimoto and Nomoto 1980, and Mazurek and Wheeler 1980).

3.1. Carbon Detonation Assumption

In the carbon detonation model, ignition of carbon grows into a thermonuclear explosion as follows.

(1) Thermal runaway into deflagration: The central temperature T_c rises developing a super-adiabatic convective core and reaches a point where the dynamical effect is essential. This critical point is defined by $\tau_n = \tau_{ff}$, where $\tau_n \equiv c_p T/\epsilon_n$ and $\tau_{ff} \equiv (24\pi G\rho)^{-1/2}$ are the nuclear timescale for a rise in temperature and the free fall timescale, respectively; the corresponding temperature is denoted as the deflagration temperature T_{def}. (The deflagration temperatures for the helium, carbon, neon, and oxygen burnings will be shown in Figure 6 and denoted by T_{def}(He), T_{def}(C), etc.) The convective URCA process (Paczyński 1972) could suppress the runaway of carbon burning initially (Iben 1978) and delay the occurence of the deflagration to somewhat higher density (Couch and Arnett 1975). Afterwards matter is incinerated into nuclear statistical equilibrium (NSE) abundances in the very central region within the free fall timescale. The temperature reaches 8×10^9K, which produces the overpressure. This is a formation of the deflagration front.

(2) Carbon detonation assumption: In the hydrodynamical model of carbon detonation (Arnett 1969; Bruenn 1971), it was assumed that the deflagration front grows into the detonation wave, i.e., the shock wave is so strong as to deflagrate the material ahead of the deflagration front. Once formed, the detonation wave propagates self-consistently (Buchler et al. 1971) while incinerating almost all materials exclusively into iron peak elements. The star is totally disrupted with the explosion energy of 1.6×10^{51}erg. It leaves no neutron star remnant and ejects 1.4 $M_\odot$ iron peak elements.

However, the assumption of the formation of a detonation wave was found to be wrong by numerical computations (Ivanova et al. 1974; Buchler and Mazurek 1975; Nomoto et al. 1976) and by semi-analytical investigation (Mazurek et al. 1977). The reason is as follows: Mazurek et al. (1977) investigated the necessary condition to initiate a Chapman-Jouguet (CJ) detonation by the shock-tube analysis. In order to form a CJ detonation at densities higher than 10^9g cm^{-3}, it is required that the nuclear energy, q, released by the deflagration is as much as the initial specific internal energy, u_0, of the degenerate matter, i.e., $q \simeq u_0$. (Hereafter the subscript 0 denotes the initial condition before the nuclear runaway occurs.) Moreover, the spherical geometry in the central region, which was not taken into account by Mazurek et al. (1977), has a large damping effect on the out-going shock wave (Ōno 1961; Lee 1972), so that

https://doi.org/10.1017/S0074180900074106 Published online by Cambridge University Press

a larger value of q/u_0 is required. On the other hand, the actual energy release for the establishment of NSE state at $\rho_c = 2.5 \times 10^9$g cm^{-3} is $q = 3 \times 10^{17}$erg/g which is only 20 percent of u_0. Therefore the resultant thermal overpressure is too small to initiate a detonation. Although q/u_0 is larger at lower densities, the carbon detonation wave is unlikely to form even at the density as low as 5×10^7g cm^{-3} (Mazurek et al. 1977).

3.2 Nucleosynthesis in Carbon Deflagration Supernovae

Without growing into the detonation, the deflagration wave propagates at a speed of v_{def} by convective energy transport across the front. Such a model was computed by Buchler and Mazurek (1975) only through a relatively early stage of the propagation and by Nomoto et al. (1976) through the explosion of the star. Nomoto et al. (1976) presented the following model of carbon deflagration supernova. The propagation velocity, v_{def}, was treated as a parameter by applying the mixing length theory of convection. Since v_{def} is slower than the sound velocity, v_s, the core expands appreciably during the subsonic propagation of the deflagration wave. Such expansion makes the deflagration weaker and, at last, quenches the nuclear burnings. In Figure 4, change in the temperature profile for the model of $v_{def} \simeq 0.2\ v_s$ is shown; the temperature decreases appreciably at late times of the propagation of the deflagration wave. Despite this quenching, the total nuclear energy release exceeds the initial binding energy, so that the star is totally disrupted.

Nucleosynthesis in the deflagration wave ($v_{def} \simeq 0.2\ v_s$) proceeds as follows.

(1) Core materials of $M_r \leq 1.03\ M_\odot$ are incinerated into NSE compositions. In the region of $1.03 < M_r \leq 1.31\ M_\odot$, partial burnings of silicon, oxygen, neon, and carbon synthesize Ca, S, Si, Ne, O, etc., in the decaying

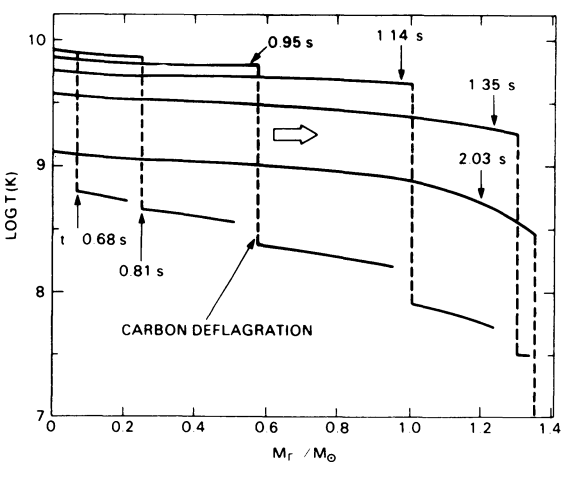

Figure 4. Propagation of the deflagration wave and change in the temperature profile.

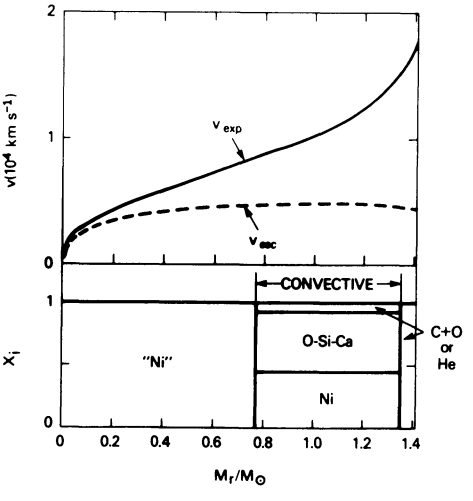

Figure 5. Chemical composition Xi, expansion velocity v_{exp}, and escape velocity v_{esc} of the carbon deflagration supernova at t = 2.03 sec.

https://doi.org/10.1017/S0074180900074106 Published online by Cambridge University Press

deflagration wave. The rest of 0.1 $M_\odot$ C+O remains unburned near the core edge.

(2) These elements are partly mixed by convection. The incinerated NSE region is convectively stable initially, i.e., entropy increases outward because energy release, q, increases along the decreasing initial density ρ_0. On the other hand, in the partially burned region of Ca-Si-O, entropy decreases outward because q decreases as the deflagration wave decays. Then the convective zone mixes the material. The convective shell expands both inward and outward so that some amount of ^{56}Ni and unburned C+O are mixed with Ca-Si-O. In Figure 5, the abundance distribution is shown at t = 2.03 s after the initiation of the deflagration. At this time, materials in the region of 0.77 $M_\odot \leq M_r \leq 1.35\ M_\odot$ are mixed. Also shown is the expansion velocity, v_{exp}, compared with the escape velocity, v_{esc}. The explosion energy in this model is $E_{expl} = 1.3 \times 10^{51}$ erg.

The abundance in the ejecta and E_{expl} depend on the assumption of the value of v_{def}. For a model of $v_{def} \simeq 0.01\ v_s$, $E_{expl} = 5 \times 10^{49}$ erg and masses or iron peak elements, partially burned Ca-Si-O, and unburned C+O are 0.16 $M_\odot$, 0.23 $M_\odot$, and 1.02 $M_\odot$, respectively.

The above features (1) and (2) are quite different from the detonation model in which materials are almost exclusively incinerated into iron peak elements. Existence of appreciable amount of Ca-Si-O mixed with iron peak elements in the carbon deflagration model is important to interpret the chemical composition of SN I by white dwarf models as will be discussed in section 5.

3.3 Type II Supernovae with Exponential Tail or Faint Supernovae

The carbon deflagration supernova with $v_{def} \simeq 0.2\ v_s$ in the intermediate mass stars would be observed as a Type II supernova (SN II) because it has an extended hydrogen-rich envelope. Moreover, it could be identified by the exponential tail in its light curve at late times because a substantial amount of ^{56}Ni provides radioactive decay energy; there exists such a kind of SN II (Weaver and Woosley 1980; Arnett 1980). If the deflagration velocity is as slow as $v_{def} \simeq 0.01\ v_s$, the explosion would be fainter than normal supernovae because its explosion energy is as small as 5×10^{49} erg.

From the point of view of nucleosynthesis, the carbon deflagration supernovae could contribute to the synthesis of iron peak elements, Ca, Si, S, O, and C in the Galaxy (cf. Wheeler et al. 1980). Their amount, however, depends on the deflagration velocity and on the lower mass limit for this mass range. This implies also that the so-called over-production difficulty of iron-peak elements in the carbon detonation model could be avoided.

4. ELECTRON CAPTURE SUPERNOVAE

4.1 Effects of Electron Capture

Electron degeneracy provides another triggering mechanism of supernova explosion in the O+Ne+Mg core of 8 to 10 $M_\odot$ stars (section 2.4), i.e., electron captures. As the core mass ($M_C \simeq M_{He}$) increases due to triple shell-burnings, ρ_c becomes so high that the electron Fermi energy exceeds the threshold energies for electron captures on ^{24}Mg and ^{20}Ne in advance of the oxygen ignition (see Figure 1).

Effects of such electron captures on evolution of the degenerate core are summarized as follows (see Sugimoto and Nomoto 1980):
(a) Trigger of the collapse: Electron captures reduce the mean mole number of electrons per one gram, Y_e, and correspondingly the Chandrasekhar limit as $M_{Ch} \propto Y_e^2$. If M_{Ch} is reduced below the core mass, the core begins to collapse (Finzi and Wolf 1967).
(b) Entropy production: From the thermodynamic point of view, electron capture produces entropy by the distortion in the electron distribution function when the mean energy of the captured electrons is less than the electron chemical potential (Bisnovatyi-Kogan and Seidov 1970; Sugimoto 1970; Nakazawa et al. 1970). Also, the gamma-ray emission from the excited states of daughter nuclei produces entropy (Rudzski and Seidov 1974).

4.2 Collapse of O+Ne+Mg Core in 8 to 10 $M_\odot$

These two effects lead to a rise in temperature and therefore the

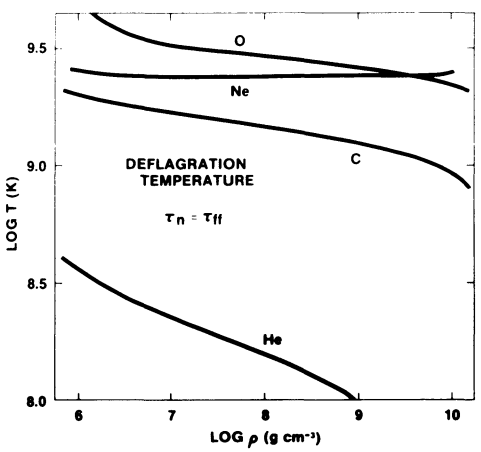

Figure 6. Deflagration temperature, T_{def}, defined at $\tau_n = \tau_{ff}$ for He, C, Ne, and O burnings.

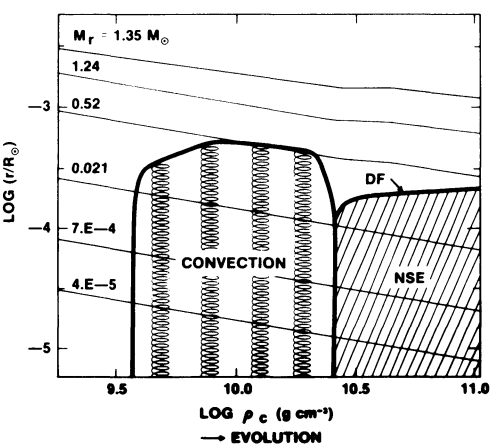

Figure 7. Quasi-dynamic contraction of O+Ne+Mg core due to electron captures on ^{20}Ne, ^{24}Mg, and NSE nuclei. Behind the oxygen deflagration front (DF), NSE region (shaded) is growing.

https://doi.org/10.1017/S0074180900074106 Published online by Cambridge University Press

oxygen deflagration will be ignited. The question is which is the final fate of this core, collapse or explosion. In order to answer this question, we need to compute the transition phase from thermal through dynamical timescale because the electron capture is a rather slow process compared with the free-fall. Miyaji et al. (1980) was the first to make such a computation from the growing phase of the O+Ne+Mg core through its collapse.

The following sequence was found to take place.

(1) Formation of a convective core and quasi-dynamic collapse: As a result of electron captures on ^{24}Mg and ^{20}Ne, the central part of the core is heated and convective core appears as seen in Figure 7. Then Y_e decreases in the entire convective core, and M_{Ch} is reduced to become almost equal to the core mass. The contraction of the core is accelerated into a quasi-dynamic collapse.

(2) Competition between electron captures and oxygen deflagration: When ρ_c reaches 2.5 x 10^{10}g cm^{-3}, oxygen burning is ignited (Figure 1). It grows into a deflagration and the material is incinerated into NSE composition. However, it does not grow into a detonation because the nuclear energy release is only 0.04 u_0. The propagation of the deflagration front (DF in Figure 7) is too slow to halt the quasi-dynamic collapse of the core. Each contracting shell is deflagrated consecutively as it is compressed to ρ = 2.5 x 10^{10}g cm^{-3}. Therefore, the DF is almost stationary in Eulerian coordinates (Figure 7).

(3) Collapse to form a neutron star: Behind the DF, the incinerated NSE region grows, from which energy is being lost by the processes of the electron captures and the photodisintegration of nuclei. Therefore, the total energy of the core is decreasing at an appreciable rate and the core continues to collapse.

4.3 Type II Supernovae Leaving Neutron Stars and Quiet Supernovae

Though Miyaji et al. (1980) stopped computing at the stage with ρ_c = 1 x 10^{11}g cm^{-3}, the core will continue to collapse and make a bounce around the nuclear density. It is likely that a neutron star is left because of the following reasons: The mass interior to the hydrogen-burning shell, i.e., O+Ne+Mg core plus thin C+O and He layers, is smaller than the limiting mass of a neutron star. The extended hydrogen-rich envelope is so weakly bounded that it would be easily blown off by the shock wave which is formed at the bounce and propagates outward to the envelope (Van Riper 1979).

The electron capture supernovae, then, would be observed as SN II leaving neutron stars. Since the death rate of stars in this mass range is appreciable, the progenitors of the observed pulsar would mostly be these stars. On the other hand, they would contribute little to nucleosynthesis, because C+O zone contains only 10^{-3} - $10^{-2}M_\odot$.

When the 8-10 $M_\odot$ star is a primary star in a close binary system, it becomes a O+Ne+Mg white dwarf by losing its hydrogen-rich envelope and then also helium envelope at their expansions (Figure 3). When this

https://doi.org/10.1017/S0074180900074106 Published online by Cambridge University Press

white dwarf accretes matter, it becomes an electron capture supernova to leave a neutron star (Nomoto et al. 1979b). Since such a supernova ejects mass of only 10^{-1} - $10^{-2}M_{\odot}$, it is called as a quiet supernova which may be required to interpret some low mass X-ray binaries.

5. WHITE DWARF MODELS FOR TYPE I SUPERNOVAE

Although several mechanisms and progenitors for SN I have been suggested, there is little agreement on the correct one (see e.g. Wheeler 1980). White dwarf is one of the candidates for SN I (e.g. Whelan and Iben 1973). Recently, Arnett (1979) and Colgate et al. (1980) have shown that the light curves of SN I can be reproduced well by the radioactive decay model ($^{56}Ni \rightarrow {}^{56}Co \rightarrow {}^{56}Fe$). This has renewed interest in white dwarf models for SN I, because it can produce a large amount of ^{56}Ni by the process of nuclear detonation or deflagration.

Supernova explosion in a white dwarf is triggered by mass accretion from a companion star in a binary system. Although a hydrogen shell flash does not grow into a supernova explosion (Starrfield et al. 1975), accretion of helium as a result of such flashes is important in terms of supernovae. Such accumulation of helium takes place when the hydrogen shell-burning is stable and steady (Sienkiewicz 1980) or when the flash is so weak that the accreted matter does not expand appreciably

Table 1. Supernovae in Accreting White Dwarfs

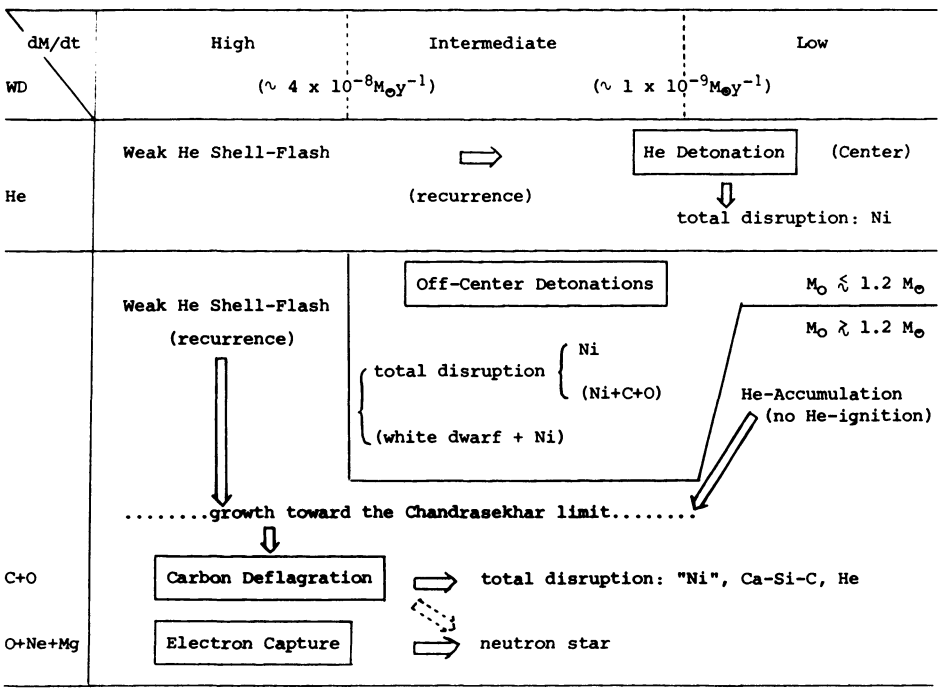

https://doi.org/10.1017/S0074180900074106 Published online by Cambridge University Press

(Shara et al. 1978). These cases are realized when the accretion rate is as high as roughly $10^{-7} M_{\odot} y^{-1}$ but is lower than at most $6 \times 10^{-7} M_{\odot} y^{-1}$ (Paczyński and Żytkow 1978; Nomoto et al. 1979a). Another possible way to build up the helium zone would be with a slow accretion of $dM/dt < 10^{-10} M_{\odot} y^{-1}$; Starrfield et al. (1980) has suggested that diffusion of CNO nuclei out of the accreted matter could then occur and lead to the stable hydrogen burning by the p-p chain.

Recently, such an accretion of helium has been investigated extensively. Several types of supernova explosions which could occur depending on the accretion rate of helium dM/dt, and initial mass M_0 and composition of the white dwarf are summarized in Table 1. Comparison with the observational data of SN I will be made in section 5.5.

5.1 Helium Detonation in Helium White Dwarfs

The triggering mechanism of the supernova explosion depends on the thermal structure in the accreting white dwarf which is set by the accretion process of helium. Such a thermal history of helium accretion was first computed by Nomoto and Sugimoto (1977) for a helium white dwarf of initial mass 0.4 $M_{\odot}$. The results depend on dM/dt as follows.

When the accretion is as high as $dM/dt = 4 \times 10^{-8} M_{\odot} y^{-1}$, helium is ignited off-center because the compressional heating due to accretion is faster than the radiative cooling in the outer layer. The shell flash is too weak to induce any dynamical effect because of such a low ignition density as $\rho = 2.7 \times 10^5$ g cm^{-3}.

When the accretion is as slow as $dM/dt = (1 - 2) \times 10^{-8} M_{\odot} y^{-1}$, on the other hand, the white dwarf is well thermally relaxed due to heat diffusion. Ignition of helium occurs in the center and is delayed until the white dwarf mass grows to $(0.8 - 1.0)\ M_{\odot}$. The helium flash is so strong that it grows into detonation, and the white dwarf is disrupted completely; the entire mass of mostly ^{56}Ni is ejected (see also Mazurek 1973). The difference from the carbon deflagration is ascribed to the difference in the energetics. In the case of helium detonation, the ratio q/u_0 is as large as 10, while $q/u_0 = 0.2$ for the carbon deflagration. Resultant shock strength is as strong as $P_{sh}/P_0 \simeq 5$ which is large enough to overcome the spherical damping and to initiate a detonation.

5.2 Off-Center Dual Detonations in C+O White Dwarfs

When the accreting white dwarf is composed of carbon-oxygen, the helium zone grows on the C+O core. Fujimoto and Sugimoto (1979) and Taam (1980a, b) computed such an accretion. They found three types of evolution depending mainly on dM/dt as schematically summarized in Table 1: When the accretion is rapid, helium flash is weak and will recur many times. For the intermediate accretion rate, the helium flash is so strong that it grows into detonation. If the accretion is slow, the final fate depends on the initial mass M_{C+O} (M_0 in Table 1) as well as dM/dt, which will be discussed in sections 5.3 and 5.4.

Hydrodynamical stages for the cases of intermediate and low accretion rates were investigated by Nomoto (1980a, b; Cases A-D) and Woosley et al. (1980; Case W). In Table 2, summarized are the parameters chosen and the numerical results, i.e., dM/dt, the initial mass of the white dwarf M_{C+O}, the mass of the accreted helium ΔM_{He} at the ignition, the density of the ignited shell ρ_{He}, q/u_0, and the explosion energy E_{expl}. In Figure 8 of ρ-T plane, evolutionary paths in the bottom of the accreted helium zone and in the center are shown for Cases A-D; when the accretion is slower, the ignition density of helium ρ_{He} is higher.

First of all, we discuss the cases of intermediate accretion rate (Cases A, B, and W). The hydrodynamic behavior for Case A is as follows. (1) Formation of the dual detonation waves: In Figure 9, changes in the temperature and pressure profiles show the formation and development of the detonation waves. Stages #1 and #4 show the post-deflagration conditions, and #2 and #3 are the post-shock pre-deflagration stages which are denoted by subscript sh. Because of high ρ_{He}, the temperature in the burning shell rises above T_{def} (He), and the materials are incinerated into NSE matter. Since q/u_0 is as high as 17, the resultant overpressure is 9 times higher than the initial pressure P_0 (#1). A shock front is formed and propagates both outward and inward (#2 and #3). Both shock waves are so strong that they grow into the helium detonation wave (He-

Table 2. Physical Quantities at the Ignition and Explosion.

Case	dM/dt ($M_\odot y^{-1}$)	M_{C+O} ($M_\odot$)	ΔM_{He} ($M_\odot$)	ρ_{He} (g cm^{-3})	q/u_0	E_{expl} (erg)
A	3×10^{-8}	1.08	0.08	2.8×10^{6}	17	1.5×10^{51}
W	1×10^{-8}	0.50	0.62	1.4×10^{7}	--	2.2×10^{51}
B	3×10^{-9}	1.08	0.23	3.6×10^{7}	3	1.9×10^{51}
C	7×10^{-10}	1.28	0.12	2.4×10^{8}	1	---
D	4×10^{-10}	1.28	0.12	(carbon ignition)		

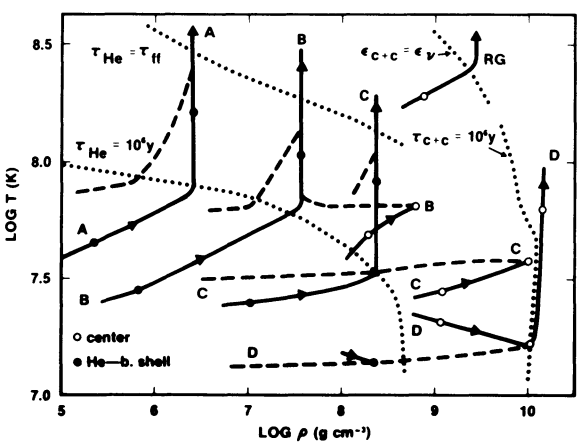

Figure 8. Evolutionary paths (solid) of the density and temperature in the bottom of the accreted helium zone (filled circle) and in the center of the white dwarfs (open circle) for Cases A-D and also for red giant stars (RG). Dashed lines are structure lines of the white dwarfs from the center toward the surface. Dotted lines are the ignition lines for He and C defined by $\tau_n = 10^6$ y and $\epsilon_n = \epsilon_\nu$. T_{def} (He) is also indicated by a dotted line.

https://doi.org/10.1017/S0074180900074106 Published online by Cambridge University Press

DW) and carbon detonation wave (C-DW), respectively; i.e., T_{sh} is higher than T_{def} (He) and T_{def} (C), respectively.

(2) Propagation of the detonation waves: In the developing phase, both detonation waves (DWs) become stronger as seen from the increasing Psh in Figure 9. Afterwards, the dual DWs propagate self-consistently with the shock strength P_{sh}/P_0 close to that of the Chapman-Jouguet detonation; even the inward C-DW was found to be strong enough to overcome the pressure gradient. In Figure 10, their propagation and the accompanying changes in the radius of Lagrangian shells are shown. The outward He-DW gives the material kinetic energy which leads to the rapid expansion. On the other hand, the materials in the C+O layers are pushed inward by the C-DW but then begin to expand. Such a pushing effect is strengthened in the very central region because the C-DW converges due to the spherical geometry. However, it is not strong enough to induce the collapse by electron captures.

(3) Disruption of the white dwarf: Both DWs reach the surface and the center, respectively, and incinerate almost all materials into NSE elements except for $10^{-3} M_\odot$ near the surface. Then, the white dwarf is totally disrupted, i.e., the entire mass of 1.16 $M_\odot$ of mostly ^{56}Ni is ejected, because the released nuclear energy is much larger than the initial binding energy. This is a supernova with $E_{expl} = 1.5 \times 10^{51}$ ergs.

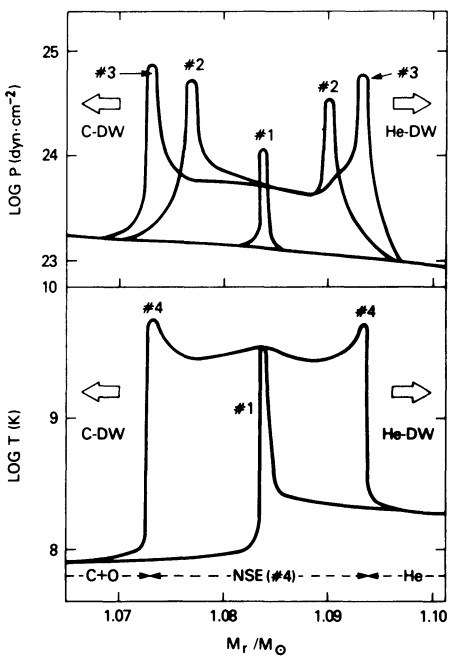

Figure 9. Formation and development of the dual detonation waves (He-DW and C-DW) for Case A.

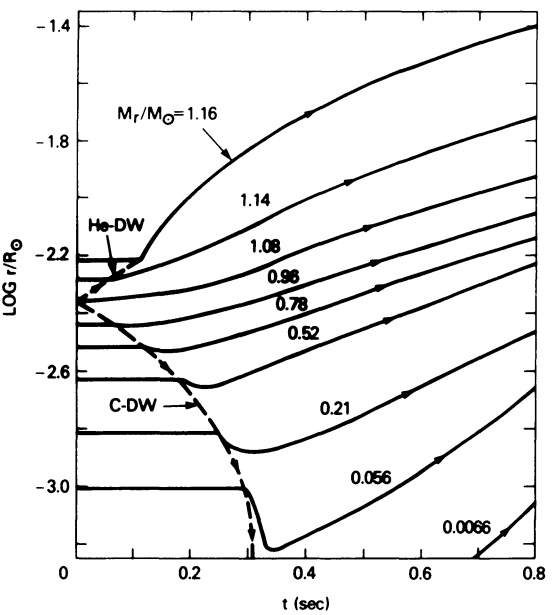

Figure 10. Propagation of the dual DWs (dashed) and the accompanying changes in the radial distance of the Lagrangian shells (solid) for Case A.

https://doi.org/10.1017/S0074180900074106 Published online by Cambridge University Press

The white dwarfs in Cases B and W also become the same type of off-center detonation supernovae. Almost all the material is incinerated into ^{56}Ni by the dual DWs except for $10^{-3}M_{\odot}$ (Case W) and $10^{-4}M_{\odot}$ (Case B). The entire mass then ejected with E_{expl} as given in Table 2.

5.3 Helium Envelope-Detonation

The dual DWs does not always form. In Case C of slow accretion, ignition of helium is delayed to a stage with $\rho_{He} = 2.4 \times 10^{8}$g cm^{-3} (Figure 8). At this density, the shock strength generated by the incineration of helium is as low as $P_{sh}/P_0 = 1.8$ because of the low q/u_0 ($\simeq$1). The resultant T_{sh} is 5×10^{8}K which is higher than T_{def} (He) but lower than T_{def} (C) as seen in Figure 6. Accordingly, the He-DW forms and propagates toward the surface while incinerating helium into NSE products. On the other hand, the C-DW does not form; in order to initiate the Chapman-Jouguet C-DW at this density, energy release, q, is required to be as much as 3 times u_0 (Mazurek et al. 1977). During the propagation of the He-DW, the C+O core remains unburned (Nomoto 1980b).

Although the computation has not yet been completed for the stages after the arrival of the He-DW at the surface, the final fate of Case C is probably as follows. Since the white dwarf mass of 1.40 $M_{\odot}$ is close to M_{Ch}, the initial gravitational binding energy in the helium zone is as large as 3.8×10^{50}erg which is slightly larger than the nuclear energy release of 3.6×10^{50}erg. This implies that some incinerated material could remain bound on the C+O core, while a part of it could be ejected. During the subsequent long phase of helium accretion, ^{56}Ni will decay into ^{56}Co and ^{56}Fe. Therefore, this white dwarf would have a Fe/He envelope above the C+O core when a supernova explosion is triggered by the carbon ignition in the center.

If the initial mass of M_{C+O} is somewhat lower than in Case C with the same accretion rate, the total energy of the white dwarf will become positive as a result of the helium incineration. Then the unburned C+O will also be ejected following after ^{56}Ni by converting the internal energy into kinetic energy. In some cases, a white dwarf remnant could be left after a rather weak supernova explosion (Nomoto 1980a).

5.4 Carbon Deflagration

There exist two possible cases of accretion for which the C+O white dwarf grows toward the Chandrasekhar limit without suffering from the off-center detonations (Table 1).

One is the case of rapid accretion. Helium flash does not grow into the detonation, and the mass of the C+O white dwarf increases as a result of the many cycles of hydrogen and helium shell-flashes. Such a white dwarf is very similar to the C+O core in red giant (RG) stars evolving through the double shell-burnings. Therefore the white dwarf evolves along a similar path as a RG in the ρ_c-T_c plane (Figure 8). Then it will explode as a carbon deflagration supernova whose outcome is similar to

https://doi.org/10.1017/S0074180900074106 Published online by Cambridge University Press

the models discussed in section 3. The ejected materials would be the mixture of iron peak elements, Ca, S, Si, O, and C.

The other is the case in which the accretion rate of helium is lower than about $1 \times 10^{-9} M_\odot y^{-1}$, and the initial mass M_{C+O} is larger than a certain critical mass (roughly 1.1 - 1.4 $M_\odot$ depending on dM/dt). Carbon is ignited in the center due to pycnonuclear reaction before helium can ignite off-center. Case D in Figure 8 shows a development of such a carbon flash (see also Taam 1980b). For smaller M_{C+O}, ρ_{He} reaches the ignition line before ρ_c reaches the ignition density of carbon (Figure 8).

Although the development of the carbon flash under such a high ignition density as $\rho_{ign} \sim 10^{10}$ g cm^{-3} remains to be investigated, the carbon deflagration supernova would be a likely outcome because ρ_{ign} is lower than the critical density (3×10^{10} g cm^{-3}) for the implosion by electron captures. In the outer layers of this type of carbon deflagration, at most 0.3 $M_\odot$ of unburned helium could be contained together with elements shown in Figure 5. In Case C, moreover, Fe could result as a product of helium envelope-detonation.

5.5 Observational Constraints on Models for SN I

Now, we will summarize the observational constraints on the theoretical models. They are the light curves and chemical compositions in the ejecta.

(1) In order to explain the peak luminosity of SN I by ^{56}Ni decay only, it is required that the amount of ^{56}Ni is as much as 1.0 - 1.4 $M_\odot$ (Arnett 1979; Chevalier 1980).

(2) Chemical compositions in the outer layers of SN I 1972e is being analyzed by Branch (1980) who compared the photoelectric scans of spectra during the thermal peak of the light curve with synthetic spectra. According to his preliminary results, the most plausible interpretation is that the outer layers of SN 1972e consisted of a mixture of Na, Ca, Si, Fe, and probably He. Abundances of such heavy elements seems to be higher than solar mass fraction. Also the upper limit to Co/Fe ratio was estimated to be about 0.1. This implies that Fe had been synthesized in the envelope before the explosion, which seems to be rather difficult to explain. (Branch (1980) noted that such a Co/Fe ratio is not yet a firm constraint in view of the present uncertainties.) Since the spectra of SN I are very homogeneous (Branch 1980), the compositions in the outer layers of most of SN I would be similar to SN 1972e.

From the theoretical point of view, there could be two types of supernova explosions in white dwarfs, i.e., detonation type (He and He/C) and deflagration type.

(1) Light curve: Both detonation and deflagration types produce large amounts of ^{56}Ni which can provide a sufficient amount of radioactive energy for the peak luminosity and exponential tail of SN I. Chevalier (1980) computed a theoretical light curve of an exploding white dwarf choosing a carbon deflagration model of $v_{def} \simeq 0.2\ v_s$ (Nomoto et al. 1976)

https://doi.org/10.1017/S0074180900074106 Published online by Cambridge University Press

as a standard model, i.e., M = 1.4 $M_\odot$ and M_{Ni} = 1.0 $M_\odot$. He showed that the theoretical light curve fits well with the observations.

The detonation type models have larger explosion energies than the deflagration models though the ejected mass is smaller, i.e., expansion velocity is larger. Then their light curves would have steeper rise and decline, i.e., shorter width for the thermal peak if the same mean opacity is assumed (Chevalier 1980). According to Barbon et al. (1973), there may exist two subclasses of SN I, i.e., slow and fast; the slow SN I has wider width and longer decline time in the light curves than the fast SN I. Therefore the deflagration and detonation type might correspond to the slow and the fast SN I, respectively. However, the light curve shape depends also on opacity and density distribution in the ejected matter so that the above suggestion needs more investigation.

(2) Chemical Composition: The ejecta of the detonation type SN is composed almost exclusively of iron peak elements; the mass of the other elements is only 10^{-4} - $10^{-3} M_\odot$. This is in conflict with the existence of S, Si, Ca, etc. in the outer layers of SN 1972e (Branch 1980). On the other hand, appreciable amount of such elements exist in the ejecta of carbon deflagration supernova. Moreover, these elements are mixed together with Ni and unburned C+O (Figure 10). Therefore the abundance feature of SN 1972e can be explained qualitatively by the carbon deflagration model (Chevalier 1980).

If we take into account the probable existence of He and high Fe abundance with a low Co/Fe ratio, the progenitor of such a SN I would be a slowly accreting white dwarf. Such a white dwarf would explode as a carbon deflagration supernova with at most 0.3 $M_\odot$ helium in the outer layers. In some cases of accretion, He and Fe could exist as a result of helium envelope-detonation to produce ^{56}Ni which decays to ^{56}Fe during the subsequent accretion of helium.

In conclusion, the carbon deflagration would be more plausible model at least for SN 1972e and probably for most of SN I rather than the detonation type from the point of view of the chemical compositions in the ejecta (Chevalier 1980). Since the white dwarf mass could grow only when the hydrogen shell-burning is stable or a weak flash, supernovae could occur only for the case of rapid or very slow accretion. Such ranges of accretion rates might preclude the detonation type but correspond to the ranges for which the carbon deflagratin occurs (Table 1).

In the white dwarf models for SN I, about 1 $M_\odot$ iron peak elements are ejected into space by each SN I. One might worry about the overproduction of iron in the Galaxy. According to Tinsley (1980), however, the production of even 1.4 $M_\odot$ iron by each SN I is not ruled out in view of the uncertainties in the star formation rate and the SN I rate.

6. CONCLUDING REMARKS

New developments of the supernova models in degenerate stars have been made for electron capture supernovae in 8 to 10 $M_\odot$ stars and the

https://doi.org/10.1017/S0074180900074106 Published online by Cambridge University Press

white dwarf models for SN I. In order to advance these models, the following problems should be clarified.

Electron Capture Supernovae: Presupernova evolution should be fully investigated: The evolution of the growing O+Ne+Mg core starting from the phase of dredging up of helium zone up to the onset of electron captures remains to be computed. Moreover, it is important to confirm the anticipation that all stars in the mass range of 8 to 10 $M_\odot$ ($\pm 1\ M_\odot$) evolve into the phase of commonly growing O+Ne+Mg core and also that several types of supernova explosion could occur for 10 to 12 $M_\odot$ stars depending sensitively on the stellar mass.

Hydrodynamical stages due to electron captures need to be studied by treating nuclear reactions and convective mixing in more detail. Problems in the core collapse and its bounce would be in common with the collapsing iron core in massive stars, although the case of a bare white dwarf might be somewhat different.

White dwarf models for SN I: Presupernova evolution, i.e., the link between the hydrogen shell-flashes and the accumulation of helium is poorly known. It depends on the several parameters in binary system (mainly on accretion rates). The relationship to the cataclysmic variables and the symbiotic stars is interesting (Nomoto 1980b).

Since the carbon deflagration supernovae seem to be the most plausible models for SN I, it is important to study the detailed nucleosynthesis by the partial burnings of Si, O, and C in the decaying deflagration wave for comparison of the chemical compositions with the observations. Appropriate treatment of the propagation of the deflagration wave due to convection is quite important. Despite the plausibility of such a deflagration model, whether the C+O white dwarf collapses or explodes (for the slow accretion in particular) is still debated; effects of convective URCA processes, critical ignition density for the implosion due to electron captures under the deflagration regime, effects of crystallization etc. are yet to be clarified.

Also other classes of models for SN I, i.e., $\sim 4\ M_\odot$ helium stars in binary systems (Arnett 1979) and $\sim 2\ M_\odot$ extended helium stars (Wheeler 1978a), need more investigation. The extended helium star should have a degenerate C+O core and explode as a carbon deflagration supernova, so that the discussions in sections 3 and 5.5 can be applied as well.

I would like to thank Prof. D. Sugmioto, and Drs. D. Branch, R.A. Chevalier, M.Y. Fujimoto, S. Miyaji, and J.C. Wheeler for stimulated discussions. Discussions with the participants in the 1980 Workshops on "Atomic Physics and Spectroscopy for Supernovae Spectra" (La Jolla), "Type I Supernova" (Austin), and "Origin and Distribution of the Elements" (Santa Cruz) were helpful to advance the present study. It is a pleasure to thank Dr. W.M. Sparks for the reading of the manuscript, useful comments, and encouragement during my stay in NASA/GSFC. This work has been supported in part by the Scientific Research Fund of the Ministry of Education, Science, and Culture of Japan (274062) and by NRC-NASA Research Associateships in 1979-1980.

REFERENCES

Alcock, C. and Paczyński, B.: 1978, Astrophys. J. 223, p.244.
Arnett, W.D.: 1969, Astrophys. Space Sci. 5, p.180.
Arnett, W.D.: 1979, Astrophys. J. Letters 230, p.L37.
Arnett, W.D.: 1980, Astrophys. J. 237, p.541.
Barbon, R., Ciatti, F., and Rosino, L.: 1973, Astron. Astrophys. 25, p.241.
Barkat, Z., Reiss, Y., and Rakavy, G.: 1974, Astrophys. J. Letters 193, p.L21.
Becker, S.A. and Iben, I. Jr.: 1979, Astrophys. J. 232, p.831.
Becker, S.A. and Iben, I. Jr.: 1980, Astrophys. J. 237, P.111.
Bisnovatyi-Kogan, G.S. and Seidov, A.F.: 1970, Astron. Zh. 47, p.139 (Soviet Astron. 14, p.113).
Boozer, A.H., Joss, P.C., and Salpeter, E.E.: 1973, Astrophys. J. 181, p.393.
Branch, D.,: 1980, in Proc. Austin Workshop on Type I Supernova, ed. J.C. Wheeler.
Bruenn, S.W.: 1971, Astrophys. J. 168, p.203.
Buchler, J.-R. and Mazurek, T.J.: 1975, Mem. Soc. Roy. Sci. Liege, 8, p.435
Buchler, J.-R., Wheeler, J.C., and Barkat, Z.: 1971, Astrophys. J. 167, p.465.
Chandrasekhar, S.: 1939, An Introduction to the Study of Stellar Structure, (Chicago: Univ. of Chicago Press).
Chevalier, R.A.: 1980, submitted to Astrophys. J.
Colgate, S.A., Petschek, A.G., and Kriese, J.T.: 1980, Astrophys. J. Letters 237, p.L81.
Couch, R.G. and Arnett, W.D.: 1975, Astrophys. J. 196, p.791.
Cox, J.P. and Salpeter, E.E.: 1964, Astrophys. J. 140, p.485.
Ergma, E.V. and Vilhu, O.: 1978, Astron. Astrophys. 69, p.143.
Finzi, A. and Wolf, R.A.: 1967, Astrophys. J. 150, p.115.
Fujimoto, M.Y. and Sugimoto, D.: 1979, IAU Colloq. No.53, White Dwarfs and Variable Degenerate Stars, eds. H.M. Van Horn and V. Weidemann, p.285.
Hachisu, I. and Sugimoto, D.: 1978, Prog. Theor. Phys. 60, p.123.
Hoyle, F. and Fowler, W.A.: 1960, Astrophys. J. 132, p.565.
Iben, I., Jr.: 1978, Astrophys. J. 226, p.996.
Ikeuchi, S., Nakazawa, K., Murai, T., Hoshi, R., and Hayashi, C.: 1972, Prog. Theor. Phys. 48, p.1890.
Ivanova, L.N., Imshennik, V.S., and Chechetkin, V.M.: 1974, Astrophys. Space Sci, 31, p.497.
Kippenhahn, R.: 1970, Astron. Astrophys. 8, p.50.
Kumar, S.S.: 1963, Astrophys. J. 137, p.1121.
Lee, J.H.: 1972, Astronaut. Acta 17, p.455.
Mazurek, T.J.: 1973, Astrophys. Space Sci. 23, p.365.
Mazurek, T.J. and Wheeler, J.C.: 1980, Fund. of Cosmic Phys., 5, p.193.
Mazurek, T.J., Meier, D.L., and Wheeler, J.C.: 1977, Astrophys. J. 213, p.518.
Miyaji, S., Nomoto, K., Yokoi, K., and Sugimoto, D.: 1980, Publ. Astron. Soc. Japan 32, p.303.
Murai, T., Sugimoto, D., Hoshi, R., and Hayashi, C.: 1978, Prog. Theor. Phys. 39, p.619.

Nakazawa, K., Murai, T., Hōshi, R., and Hayashi, C.: 1970, Prog. Theor. Phys. 44, p.829.
Nomoto, K.: 1980a, in Proc. Austin Workshop on Type I Supernova, ed. J.C. Wheeler.
Nomoto, K.: 1980b, in Proc. IAU Colloq. No.58, Stellar Hydrodynamics.
Nomoto, K. and Sugimoto, D.: 1977, Publ. Astron. Soc. Japan 29, p.765.
Nomoto, K., Sugimoto, D., and Neo, S.: 1976, Astrophys. Space Sci, 39, p.L37.
Nomoto, K., Nariai, K., and Sugimoto, D.: 1979a, Publ. Astron. Soc. Japan 31, p.287.
Nomoto, K., Miyaji, S., Yokoi, K., and Sugimoto, D.: 1979b, IAU Colloq. No.53, White Dwarfs and Variable Degenerate Stars, eds. H.M. Van Horn and V. Weidemann, p.56.
Ōno, Y.: 1960, Prog. Theor. Phys. 24, p.825.
Paczyński, B.: 1970, Acta Astron. 20, p.47.
Paczyński, B.: 1971, Acta Astron. 21, p.271.
Paczyński, B.: 1972, Astrophys. Letters 11, p.53.
Paczyński, B. and Żytkow, A.N.: 1978, Astrophys. J. 222, p.604.
Rakavy, G., Shaviv, G., and Zinamon, Z.: 1967, Astrophys. J. 150, p.131.
Rose, W.K.: 1969, Astrophys. J. 155, p.491.
Rudzskii, M.A. and Seidov, Z.F.: 1974, Astron. Zh. 51, p.936. (Soviet Astron. 18, p.551).
Shara, M.M., Prialnik, D., and Shaviv, G.: 1978, Astron. Astrophys. 61, p.363.
Sienkiewicz, R.: 1980, Astron. Astrophys. 85, p.295.
Starrfield, S., Truran, J.W., and Sparks, W.M.: 1975, Astrophys. J. Letters 198, p.L113.
Starrfield, S., Truran, J.W., and Sparks, W.M.: 1980, submitted to Astrophys. J. Letters.
Sugimoto, D.: 1970, Astrophys. J. 161, p.1069.
Sugimoto, D. and Nomoto, K.: 1975, Publ. Astron. Soc. Japan 27, p.197.
Sugimoto, D. and Nomoto, K.: 1980, Space Sci. Rev. 25, p.155.
Taam, R.F.: 1980a, Astrophys. J. 237, p.142.
Taam, R.F.: 1980b, submitted to Astrophys. J.
Tinsley, B.M.: 1980, in Proc. Austin Workshop on Type I Supernova, ed. J.C. Wheeler.
Van Riper, K.A.: 1979, Astrophys. J. 232, p.558.
Weaver, T.A. and Woosley, S.E.: 1979, Bull. AAS 11, p.724.
Weaver, T.A. and Woosley, S.E.: 1980, in Proc. La Jolla Workshop on Atomic Physics and Spectroscopy for Supernovae Spectra, ed. R.E. Meyerott.
Wheeler, J.C.: 1978a, Astrophys. J. 225, p.212.
Wheeler, J.C.: 1978b, Mem. della Soc. Astron. Italiana 49, p.349.
Wheeler, J.C. (ed.): 1980, Proceeding of the Workshop on Type I Supernova, 17-19 March 1980, Univ. of Texas at Austin, in press.
Wheeler, J.C., Miller, G.E., and Scalo, J.M.: 1980, Astron. Astrophys. 82, p.152.
Whelan, J. and Iben, I., Jr.: 1973, Astrophys. J. 186, p.1007.
Woosely, S.E., Weaver, T.A., and Taam, R.F.: 1980 in Proc. Austin Workshop on Type I Supernova, ed. J.C. Wheeler.

DISCUSSION

Sugimoto: You discussed a model in which the helium and carbon detonation waves propagate both ways. As the carbon detonation wave propagates inwards, the pressure of the ambient matter, i.e., the average pressure, increases very greatly and the shock strength should decrease considerably. How far inwards does the front continue to be detonation wave?

Nomoto: The inward-moving detonation wave is weakened by the initial pressure gradient and strengthened by the spherical geometry in the central region. In our model, the nuclear energy release is large enough compared with the initial internal energy of the matter to overcome the damping effect of the pressure gradient. Although the shock strength decreases, it is still as large as about 4 when the detonation wave reaches the shell with a mass fraction of $M_r/M \simeq 0.2$; the detonation wave is therefore self-consistent there. After that, the inward detonation wave grows due to the focusing effect of the spherical geometry. The pressure in the centermost region increases by a factor of 300. So, one might expect that a collapse would be triggered by the inward-moving shock wave. In our model, however, the mass of the highly compressed region is only 3×10^{-4} $M_\odot$ which is too small to trigger the collapse.

Mazurek: One small comment regarding your point that the less tightly bound outer envelope of your electron capture supernova model may help to give an explosion. The present problem in getting a supernova from collapse in hydrodynamic calculations is getting the shock to propagate to the surface of the compact core that initially collapses. An inner region of the initial core having less than one solar mass collapses homologously and bounces. The shock that forms at its surface is not able to travel through the remaining 0.4 $M_\odot$ of collapsing initial core before it dies out. The problem for mass ejection therefore seems to be at the higher densities within the original degenerate core ($M \sim 1.4$ $M_\odot$). The less tightly bound envelope exterior to the core therefore may be of little help.

Nomoto: The propagation of the reflected shock wave may depend on the equation of state at high densities.

Wheeler: Although I think your model for producing iron on top of a carbon core has some problems with insufficient helium at explosion, I would like to congratulate you on your ingenuity in suggesting a picture that is at all plausible. When we last talked, this was a point of great confusion. Concerning the models of Type I supernovae, there are still many problems. For instance, Chevalier's model, in which the whole light curve is produced by radioactivity, is simultaneously too dim at maximum and too bright in the exponential tail. This problem can not be solved by scaling the amount of ^{56}Ni. Some shock energy at maximum, and hence an extended envelope, may be necessary.

https://doi.org/10.1017/S0074180900074106 Published online by Cambridge University Press